

Conditional scalar dissipation rates in turbulent wakes, jets, and boundary layers

P. Kailasnath, K. R. Sreenivasan, and J. R. Saylor
Mechanical Engineering Department, Mason Laboratory, New Haven, Connecticut 06520-8286

(Received 10 August 1992; accepted 20 July 1993)

The expected value $E_\chi \equiv E(\chi, \theta = \theta_0)$ of the dissipation rate χ of a passive scalar θ conditioned on the scalar value $\theta = \theta_0$ has been measured in three varieties of turbulent shear flows: heated wakes, dyed liquid jets, and the atmospheric surface layer. The quantity E_χ depends fairly strongly on θ_0 and on the flow. For the wake, E_χ exhibits two peaks—one on the low-temperature end and the other on the high-temperature end—and the peaks are separated by an approximately flat region. The relative strength of the two peaks varies with the spatial position. Measured in the turbulent part alone, E_χ tends to have only one peak on the hot side, but is still nonuniform. The related quantity, $E_{\theta''} \equiv E(\nabla^2 \theta, \theta = \theta_0)$, which is the expected value of the Laplacian of the scalar conditioned on the scalar concentration, has also been measured on the wake centerline and shows a simpler dependence on θ_0 than E_χ . For jets, E_χ has a single peak on the high-concentration side. This feature appears to be essentially independent of the use of Taylor's hypothesis and on whether or not the dissipation rate χ is approximated by only one of its components. It is, however, sensitive to the resolution of measurement. For the temperature fluctuation in the atmospheric boundary layer, the peak in E_χ on the cold side is far weaker than that on the hot side. From this combination of experiments, it is argued that the different shapes of E_χ in different flows are related to differences in the nature of the scalar pdf itself and, for the high-Schmidt-number dyes in water flows, on whether or not the finest scales of the scalar are resolved.

I. INTRODUCTION

The equations describing the evolution of the probability density function (pdf) of a passive scalar θ mixed by turbulence require closure for the expected value of the scalar dissipation rate, χ , conditioned on the concentration of the scalar itself. We shall designate the conditional expectation of the dissipation rate at concentration θ_0 by $E_\chi \equiv E(\chi, \theta = \theta_0)$. Another quantity of equal interest is $E_{\theta''} \equiv E(\nabla^2 \theta, \theta = \theta_0)$, which is the expected value of the Laplacian of θ conditioned on the scalar concentration. References 1–5 serve as good source material for pdf closure methods for passive scalar fluctuations.

The general notion that the small scale features of turbulence are independent of the large-scale leads to a model where E_χ is independent of θ_0 . It has been pointed out repeatedly^{1–3} that for homogeneous turbulence, this independence is a necessary and sufficient condition for the pdf of θ , $p(\theta)$, to be Gaussian. Eswaran and Pope⁶ have numerically examined the evolution of E_χ from some prescribed state in isotropic and homogeneous turbulence at a microscale Reynolds number of 50, and found that their asymptotic distribution depends on the scalar concentration. Gao and O'Brien⁹ have discussed the qualitative features of the correlation between the scalar and its gradient, and concluded that the most important contribution to this correlation comes from initial conditions.

Even though progress has occurred in several directions, the need for experimental data on these conditional quantities cannot be overemphasized. It is difficult to measure them exactly (see Ref. 10 and Sec. IV) because of the demands imposed on three-dimensional spatial resolution

and the extent of the data base required for convergence. However, it is not so difficult to measure them under the following assumptions: (a) The dissipation can be approximated, omitting a constant multiplicative factor, by one of its components, $(\partial\theta/\partial x)^2$, with x as the direction of the main stream, and (b) the space derivative in the x direction can be obtained by invoking the so-called frozen flow hypothesis due to Taylor, according to which turbulence convects without distortion in the direction of the local mean velocity. In spite of much work (e.g., Refs. 10–12), the realism involved in assumption (a) is unclear but there are reasonable indications that several average properties of the total scalar dissipation can be gauged from those of one component. There are also indications (e.g., Refs. 13–15) that Taylor's hypothesis is a reasonable approximation at least in regions of low turbulence activity. Recently, Jayesh and Warhaft¹⁶ have measured the conditional dissipation rate in grid-generated turbulence under the assumptions stated above. However, most turbulent flows are inhomogeneous and anisotropic, and the scalar pdf in these flows is distinctly non-Gaussian. In fact, several experiments (see, for example, Ref. 17) suggest that the global features of scalar gradients may be influenced measurably by the large-scale features of a turbulent flow. Thus, in general, E_χ would be expected to depend on θ_0 and, perhaps, on the flow itself.

In this paper, the conditional expectation of E_χ is measured for two turbulent flows at moderate Reynolds numbers (the temperature field in a heated wake behind a circular cylinder and the fluorescing dye field in a round jet) as well as for the temperature field in the atmospheric surface layer at a high Reynolds number. For the wake, the

data are presented under the assumptions (a) and (b). The conditional expectation $E_{\theta'}$ has been obtained, for the wake centerline, by direct measurement, as well as from E_{χ} under the assumption of homogeneity. The agreement between the two estimates can be thought to justify the assumption of homogeneity on the wake centerline. In general, $E_{\theta'}$ is better behaved than E_{χ} . For the jet flow which is especially vulnerable to the assumption (b), E_{χ} has been measured with and without that assumption. Furthermore, the assumption (a) has been relaxed to various degrees and the consequences are explored. The effect of the measurement resolution is also investigated. High-Reynolds-number data on E_{χ} from a neutrally stable atmospheric surface layer are also included. From this combination of experiments, an attempt has been made to answer a variety of questions relating to the dependence of E_{χ} on θ_0 , as well as the flow, the effect of Taylor's hypothesis, the effect of using a component of χ instead of the sum of its three components, the effect of poor resolution of measurement, and so forth. It is argued that the different shapes of E_{χ} in different flows are related to differences in the nature of the scalar pdf itself and, for the high-Schmidt-number dyes in water flows, on whether or not the finest scales of the scalar are resolved.

II. EXPERIMENTS

The turbulent wake was created in a suction-type subsonic wind tunnel with a cross-sectional area of 72×56 cm. The cylinder had a diameter of 1.9 cm and spanned the tunnel width of 76 cm (aspect ratio=38). The cylinder was heated uniformly by internal heating elements. Measurements were made at the farthest downstream location where the influence of the tunnel walls was not felt. This turned out to be about 80 diam behind the cylinder. Detailed measurements across the wake, including its centerline, were made at $R_d=5300$, where R_d is based on the upstream velocity and the cylinder diameter, d . This is designated as wake L . The centerline was determined by measuring the profiles of mean and fluctuating temperature at several streamwise positions in the wake. The wake development with heating was quite close to that for unheated wakes as reported, for example, in Ref. 18. Heating did not produce conspicuous changes at the measurement location, where the maximum excess temperature was 2 °C. The estimated Kolmogorov scale on the centerline was about 0.43 mm. Since the Prandtl number for air is about 0.72, the dissipating scale for the temperature is about 0.55 mm.

Temperature fluctuations were measured by means of a 0.5 mm long, $0.6 \mu\text{m}$ diameter cold wire operated on a constant current anemometer operated at a current of 120 μA . The low operating current means that the velocity contamination is small (though nonzero). The length of the cold-wire is about twice the Kolmogorov scale, and thus some averaging takes place in the direction of the wire length. The anemometer, built-in house, was based on a design by Peattie.¹⁹ The fidelity of the cold wire, as estimated from previous studies on the frequency response of similar wires, was taken to be about 4 kHz; this was fairly

close to the estimated scalar dissipation frequency of about 6.6 kHz. The noise floor in the measurements occurred around 4 kHz. The signal from the cold wire was therefore filtered at 4 kHz and sampled at 8 kHz using a 12 bit digitizer. Ten data files, each consisting of 512 000 points, were obtained.

Measurements were also made on the wake centerline at a cylinder Reynolds number of 20 000 (wake H). Although the results for wake H were found to be quite similar to those of wake L , they are not presented here because the spatial and temporal resolutions fell short of the Kolmogorov scale. However, we used the data to explore qualitatively the Reynolds-number dependence of E . In particular, for accurately obtaining the tails of the pdf's on the centerline, we used very long records of 200 million data points equivalent to about 15 hrs of real-time data acquisition.

One of the turbulent jets (designated R) was produced by allowing water to flow from a settling chamber through a nozzle of circular cross section (diameter $D=1.2$ cm) into a tank of still water at a constant speed of 35 cm/sec. The nozzle was contoured according to a fifth-order polynomial to have zero slope and curvature at the entrance and the exit. The upstream flow management techniques were standard. The jet Reynolds number based on nozzle diameter and exit velocity was about 3900. Data were acquired on the jet centerline at 37 diam downstream of the nozzle. (In contrast to the wake, the jet centerline was *assumed* to be the geometric axis of symmetry.) The estimated Kolmogorov and Batchelor scales at the measuring station were estimated to be about 160 and $4 \mu\text{m}$, respectively.

To test the effect of Taylor's hypothesis, use has been made of the earlier spatial data²⁰ of the concentration field in jet R . These data are in the form of two-dimensional images of the scalar field between 10 and 21 diam downstream of the nozzle, obtained by the planar laser-induced fluorescence techniques. Briefly, the light beam from a YAG laser was formed into a sheet of the order of $250 \mu\text{m}$ thickness, and made to intersect the jet mixed with small amounts of a fluorescing dye (see below). The laser-induced-fluorescence images were then obtained on a Photometrics CCD array (size 1300×1024) with a pixel resolution of the order of $150 \mu\text{m}^2$. More details can be found in Ref. 20.

A second water jet (designated J) was produced at a somewhat smaller Reynolds number of 2700 using a nozzle of 1.6 mm diameter and exit velocity of 170 cm/sec. The general arrangement of the two flows was similar. Measurements were made at 147 diam downstream of the nozzle. These measurements were made to complement those of jet R because of our concern that the latter might not be far enough from the nozzle exit to have attained self-preservation. The estimated Kolmogorov and Batchelor scales are 160 and $6 \mu\text{m}$, respectively.

The jets were mixed with small amounts of disodium fluorescein, and fluctuations in its concentration were measured optically; for jet J , another dye (basic blue 3) was also used. The incoming radiation was from a continuous

wave argon-ion laser at the wavelength of 488 nm. The peaks in the fluorescing spectra were at 515 nm for the fluorescein and 670 nm for the basic blue 3. In both cases, the linearity of the optical signal, with respect to the dye concentration has been checked carefully,²¹ the influence of photobleaching of the dye was also investigated, and was found not to affect the present results beyond other uncertainties discussed later.

For jet *R*, attempts were made to resolve the Batchelor scale. The optical setup used and the measurement procedure were discussed in Ref. 22. Briefly, various combination of lenses was used to focus a light beam to a spot of about 6 μm diameter. In the path of the photomultiplier tube which records the fluctuations, additional lenses were located to give an image enlargement by a factor of 2.5. This combination enlarges the 6 μm focal spot in the flow to a size of about 15 μm . Ahead of the photomultiplier tube, a 10 μm diameter pinhole was located which effectively reduces the spot imaged on to the phototube to 4 μm , this being the nominal spatial resolution. (The numbers quoted here were calculated using laws of optics in air. In practice, the diameter of the spot in water is somewhat bigger, but the resolution remains to be on the order of the Batchelor scale.) For jet *J*, no attempts were made to resolve the Batchelor scale: The linear dimension of the measurements volume was on the order of 32 μm —more than enough to resolve the Kolmogorov scale—and the optical arrangement was standard in most respects.

The optical signal from the photomultiplier tube was passed through a current amplifier before digitizing the data on the MASSCOMP computer. For jet *R*, the digitizing frequency was set to 320 kHz, which is well below the limiting digitizing rate of 1 MHz of the A/D converter. The photomultiplier tube is believed to have frequency fidelity of up to 50 MHz, so that the temporal response of the instrumentation is much better than is required for the purpose. Record lengths were of the order of 1 second real time. For jet *J*, the sampling frequency was 32 kHz, and the record lengths were of 5 sec duration.

The atmospheric temperature data were acquired using the cold wire instrumentation described earlier. Measurements were made at a height of 2 m above the roof of a four storey building, as well as about 6 m in the field over a wheat field canopy in the Connecticut Agricultural Research Station about 10 miles north of the Yale campus. No systematic stability conditions of the atmosphere were recorded. Since the roof and field data yielded similar results (thus assuring us that differences in the fetch and perhaps atmospheric stability were nonessential), it is thought that the presentation of one set of results is enough. We choose to present the roof data. In this instance, the signals were low pass filtered at 800 Hz and sampled at 2.4 kHz. The digitized data were acquired on an IBM PC, and consisted of 13 files, each consisting of 180 000 points. Because of the usual low-frequency variations in atmospheric flow conditions, results have been presented as averages over several files. The file combinations have been designated as *L*, *M*, and *H* in the order of the increasing stringency regarding the uniformity of mean ve-

locity conditions while selecting files within a group. It is worth pointing out right away that the conclusions are essentially independent of the combinations used.

III. RESULTS FOR THE WAKE

A. Pdf of the scalar

Figure 1(a) shows, for the turbulent wake *L*, the pdfs of temperature Θ normalized by the local root-mean-square (rms) value Θ' . (Note: We use θ to indicate a passive scalar generically, Θ to denote the temperature, and c to denote the concentration.) Different curves correspond to different transverse locations across the wake. The pdf on the centerline is unimodal, whereas those measured away from the centerline show a bimodal feature with sharp narrow spikes at the cold end. This spike is due to the presence of the cold outer fluid at the off-center positions of the wake.^{23,24} The differences in the location of the spike at the various transverse locations is due to differences in the mean and rms temperatures at these locations. Figure 1(b) shows the pdf's of the temperature fluctuations without normalizing by the respective rms values. The origin for the temperature coordinate in Fig. 1(b) is the mean centerline temperature in the wake.

Figure 1(c) is a replot of Fig. 1(b) in logarithmic coordinates, so as to accentuate the tails of the distributions. This figure shows the pdf at the centerline of the wake has a cutoff at the room temperature. There is therefore some low level of intermittency also on the centerline of the wake. The "cold" side of the centerline pdf exhibits a sizeable exponential part (with abrupt termination at the outside free-stream temperature), while on the hot side the pdf is closely Gaussian. This striking difference between the two sides indicates that the dominant phenomena are different on the two sides. Although this is not a central issue for this paper, it is worth remarking that exponential and Gaussian pdf's can be formally predicted by extending the theory proposed by Sinai and Yakhot⁷ and Yakhot.²⁵ Roughly speaking, contributions to the hot side are from the well-mixed turbulent upstream fluid in the wake (essentially reflecting the dynamics of decaying turbulence) and those to the cold side are from the cold unmixed fluid from the potential stream penetrating the interior of the wake.

B. Conditional expectation $E(\chi, \Theta = \Theta_0)$

Figure 2 shows the plots of the conditional distribution $E(\chi, \Theta = \Theta_0)$ across the wake. The distribution is quite nonuniform, contrary to the situation that would occur if small scales were independent of the large scales. The peak at the cold end converges quite well, while the convergence on the hot end is rather poor even though very long data records have been used. The reason appears to be that the coldest temperatures are limited by the room temperature while the temperature at the hot end, corresponding to the fluid elements arriving from the upstream of the measurement station, are not so well defined; in general, the longer one waits, the larger is the hottest temperature measured

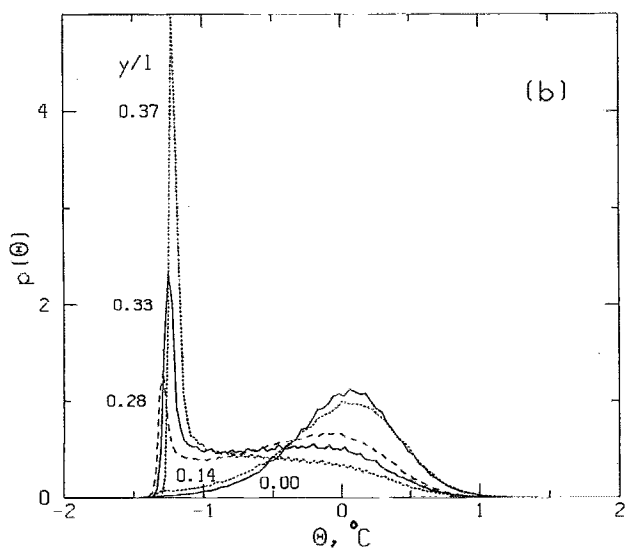
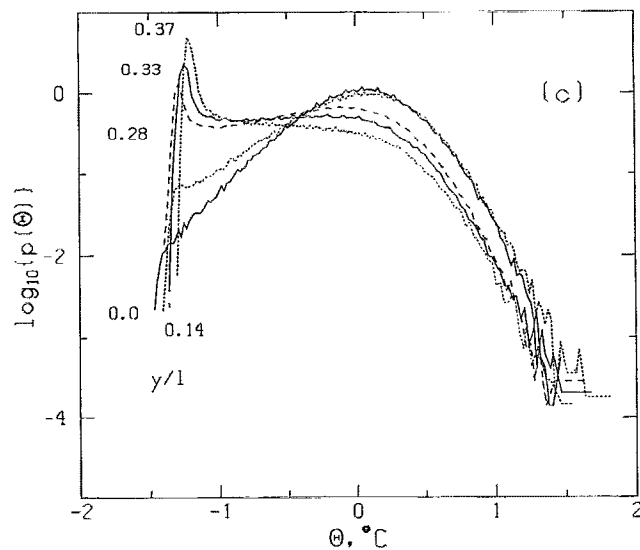
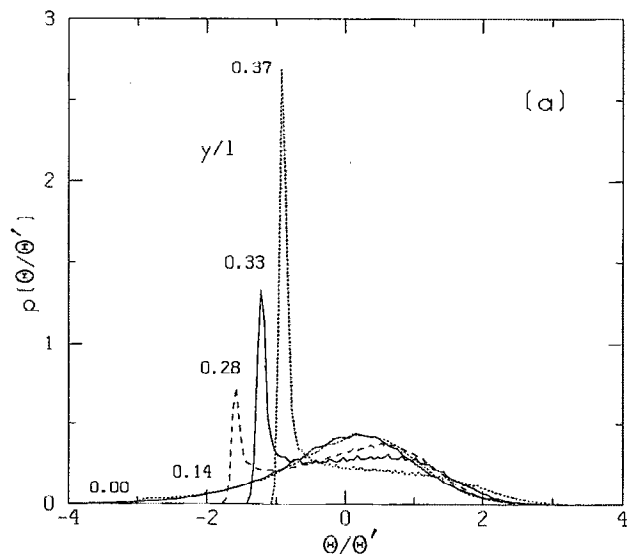


FIG. 1. The probability density function of the temperature fluctuations in the wake of a heated cylinder at different positions across the wake. $x/d=78$ and $R_d=5300$. For (a), the abscissa is the temperature normalized by its rms value. For (b), the temperature is given in $^{\circ}\text{C}$ and referenced to the mean centerline temperature. (c) is the same as (b) except that the probability density is plotted in logarithmic coordinates. The nomenclature is the same for all three figures.

by the probe. (The hottest temperature possible is, of course, that very near the cylinder. This temperature is many tens of standard deviations larger than the mean temperature at the measuring station, and is therefore most unlikely to be experienced there.) Different temperature records will therefore show significant variations in the hottest temperatures. Even very long records of 200 million data points for wake H (see Sec. II) extend the pdf of the temperature fluctuations to 5.5 rms and do not show any evidence of convergence at the uppermost end. We conclude that the *dominant* reason for the poor convergence at the hot end is the *inherent lack of definition* of the hottest temperature. (We cannot completely rule out the possibility that a more definite cutoff may occur, say, an order of magnitude farther downstream than is the case here, but this seems unlikely. In any case, reliable measurements so far downstream are very difficult because of the extremely low signal to noise ratio.)

The nature of the cutoff at the two extreme temperatures must now be discussed. The coldest fluid is the unmixed fluid from the potential stream. The temperature

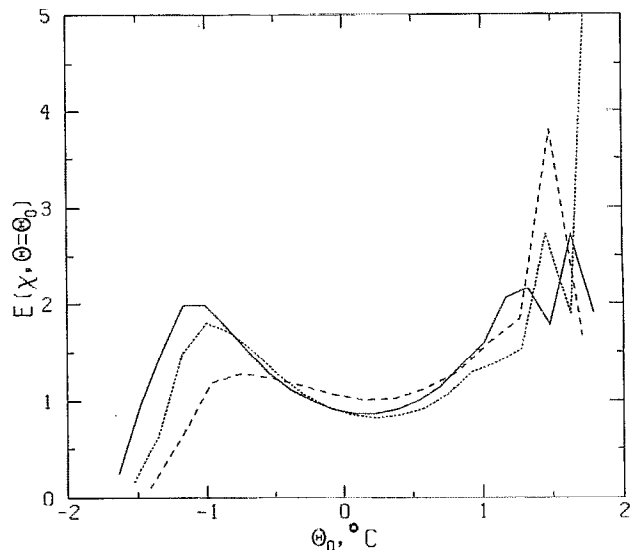


FIG. 2. Conditional expectation of the scalar dissipation across the wake of a heated cylinder. —, $y/l=0$; \cdots , $y/l=0.13$; ---, $y/l=0.28$. Here, $l=(xd)^{1/2}$.

dissipation in that fluid is expected to be zero, resulting in the observed cutoff. This cutoff point is unique for a given flow. On the hot end, on the other hand, temperatures larger than those registered in the present record length will undoubtedly occur if the data record length were even longer, though it is bound to occur with even lower probability. The intuitive expectation of large dissipation for these low-probability events suggests that on the hot side E_χ should increase with Θ . The cutoff point for any record length appears to be abrupt, but it is not unique for reasons already mentioned. We thus believe that the very hot events associated with very high intermittent dissipation rates are nonuniversal. The low temperature events could also be expected to be nonuniversal, but they would not contribute much to E_χ at the cold end because the dissipation in the cold fluid is small anyhow. In fact, the quantity E_χ at the outer locations, being dominated by the cold fluid with low temperature gradients, diminishes the magnitude of cold lobes. The limiting shape of the off-center distribution can therefore be expected to be roughly unimodal due to the disappearance of the peak on the left. This is indeed the case. In general, however, E_χ can be thought to consist of two lobes—one of which is due to contributions from the potential cold fluid juxtaposed with the turbulent fluid, and the other is due to contributions from the fully turbulent hot fluid from upstream. The former would generally be associated with a significantly lower $E(\chi, \Theta = \Theta_0)$ than the latter. The precise shape of E_χ depends on the relative strengths and the mechanisms of the two contributions.

C. Conditional expectation $E(\nabla^2\Theta, \Theta = \Theta_0)$

As remarked in Sec. I, the molecular term in the evolution equation for the $p(\Theta)$ can alternatively be written in terms of the conditional quantity $E_{\Theta''} \equiv E(\nabla^2\Theta, \Theta = \Theta_0)$. Even though one can obtain $E_{\Theta''}$ from E_χ for homogeneous flow by simply noting²⁶ that $(d/d\Theta_0)(pE_\chi) = (pDE_{\Theta''})$, D being the diffusion coefficient, it would be useful to evaluate $E_{\Theta''}$ directly—largely as a check on the homogeneity assumption. Only the centerline wake data were processed in this fashion. Figure 3 shows a comparison between the $E_{\Theta''}$ obtained directly and that inferred from E_χ of Fig. 2 using the assumption of homogeneity. The close agreement over most of the temperature values is an indication that this assumption is reasonable on the wake centerline, at least for temperatures which are not too low. The relatively large differences at low temperatures do not seem unreasonable because of their association with the outer fluid (see Fig. 1 and text). Note that the distribution of $E_{\Theta''}$ is simpler than that of E_χ .

IV. RESULTS FOR THE JET

A. The effect of using a single component of χ

To assess qualitatively the effects of using a single term of χ instead of the sum of its three components, the scalar dissipation for jet R was estimated in three different ways from the two-dimensional spatial maps of the concentration field: (i) $\chi = (dc/dx)^2$, (ii) $\chi = (dc/dy)^2$, (iii) $\chi = (dc/dx)^2 + (dc/dy)^2$, where x and y are the axial and

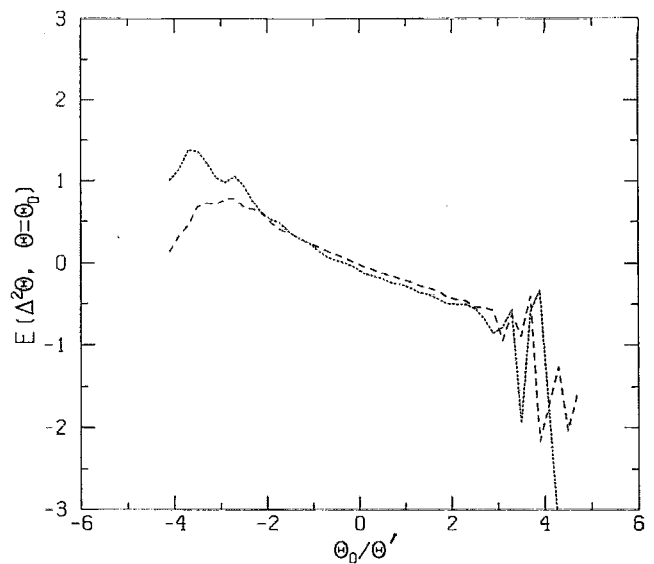


FIG. 3. Conditional expectation of the Laplacian of the scalar on the centerline of the wake. $x/d=78$, $R_d=5300$. ---, computed directly; ···, computed from E_χ for the wake centerline, Fig. 2.

radial coordinates, respectively. All estimates were obtained with spatial resolution of the order of the estimated average Kolmogorov scale. Typical regions of the jet where the χ data were obtained are marked in Fig. 4; we used the concentration data from several such nonintermittent re-

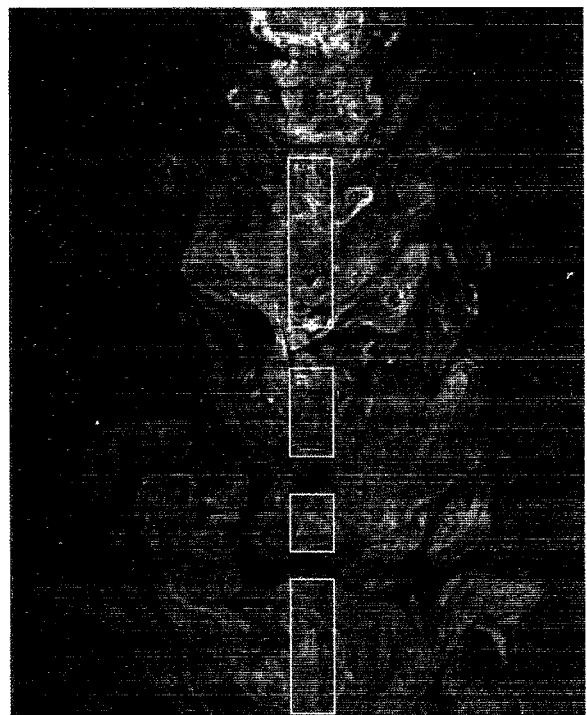


FIG. 4. A realization of the two-dimensional cross section of jet R . The boxes marked in the figure are typical of fully turbulent, nonintermittent regions where the conditional expectation was computed. Several such boxes from several realizations were used for computing the conditional expectation.

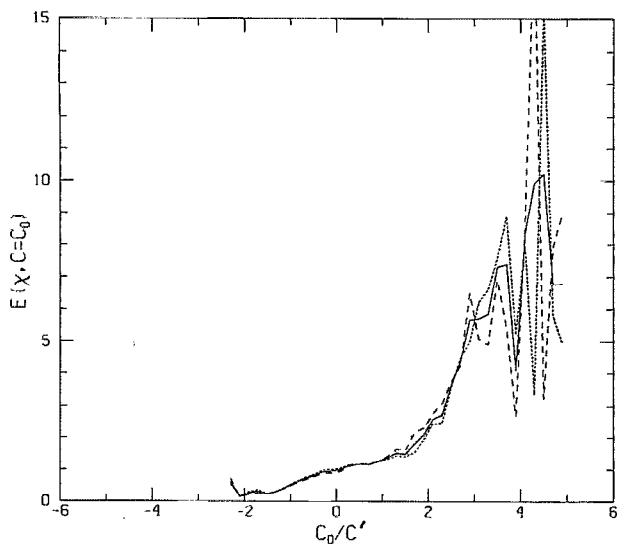


FIG. 5. Comparison of the conditional expectation from spatial data of jet R taken from regions such as marked in Fig. 4. The three curves correspond to the following three different ways of approximating χ : For the full-line curve, χ is approximated by $(dc/dx)^2 + (dc/dy)^2$; ---, $\chi = (dc/dx)^2$; \cdots , $\chi = (dc/dy)^2$.

gions from several realizations of the jet. The results on E_χ are shown in Fig. 5. Unlike the wake data, the distributions are single lobed, an aspect to which we shall presently return. The three curves are fairly close to each other, except that the sum (iii) above yields less violent variations on the high end. In general, it might be said that the overall shape of E_χ is nearly insensitive to how χ is estimated. We therefore conclude that using a single component is acceptable in accuracy for estimating the overall shape of E_χ .

In obtaining E_χ from spatial data, we tested the sensitivity to the streamwise position by choosing boxes at different distances from the nozzle. Our tentative conclusion is that this does not play a crucial role. We shall briefly return to this aspect once again.

B. The effect of Taylor's hypothesis on the measurement of E_χ

The jet flow is especially vulnerable to deficiencies of Taylor's hypothesis because of the relatively large turbulence intensities. In order to see how Taylor's hypothesis might distort the results, $E(\chi, c=c_0)$ obtained from temporal data for jet R are compared in Fig. 6 with the appropriate spatial data of Fig. 5. The comparison is satisfactory for low concentration levels, but there are significant differences on the high end (where, for other reasons as well, the precise shape of E_χ is uncertain). The conclusions from measurements in jet J are similar, thus demonstrating that the sensitivity of the shape of E_χ on the streamwise position is not strong.

C. The effect of measurement resolution

Together, the two earlier tests shed some light on the validity of assumptions (a) and (b) of Sec. I. We now examine the effect of measurement resolution by analyzing

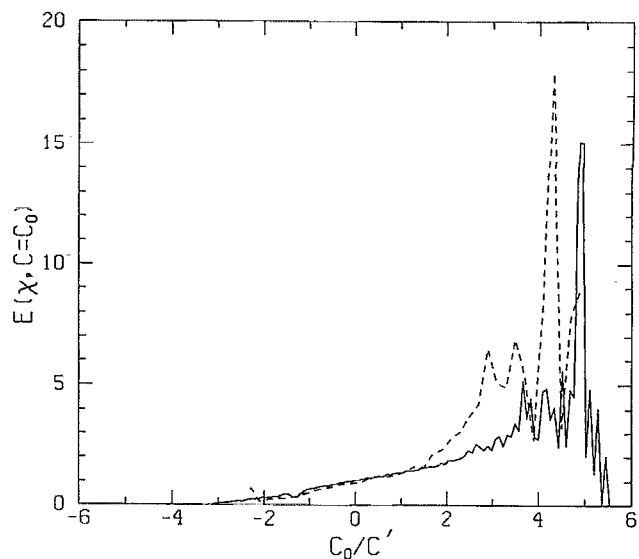


FIG. 6. Conditional expectation of the scalar dissipation on the centerline of jet R . $x/d=37$, and $R_d=3900$. The concentration is normalized by its rms value. The spatial resolution is of the order of the Kolmogorov scale. ---, without Taylor's hypothesis, $\chi = (dc/dx)^2$; \cdots , with Taylor's hypothesis, $\chi = (dc/dx)^2 \sim (dc/dt)^2$.

the temporal data obtained on the jet centerline. (As already remarked, the centerline is only nominal, and the possibility that the measurement station was *somewhat* off center cannot be ruled out.)

Figure 7 shows for the centerline of water jets the distribution of $E(\chi, c=c_0)$. Both curves are for jet R and are obtained by using assumptions (a) and (b) of Sec. I, but one of them is obtained with resolution of the order of the Kolmogorov scale and the other with the Batchelor scale

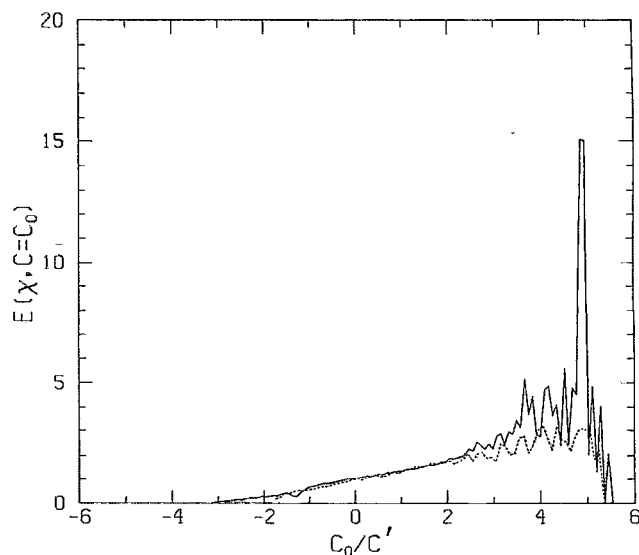


FIG. 7. Conditional expectation of the scalar dissipation on the centerline of jet J . Taylor's hypothesis is used and χ is approximated in each case by $(dc/dx)^2 \sim (dc/dt)^2$. The concentration is normalized by the rms value. The measurement resolution is of the order of the Kolmogorov scale for —, and of the order of the Batchelor scale for \cdots .

resolution (see Sec. II). The two curves are nearly identical at the low concentration end, but differ significantly on the high concentration end, with a somewhat smoother behavior exhibited by the data resolving the Batchelor scale. This appears reasonable because the dissipation estimates based on resolutions of the order of the Kolmogorov scale show intense (and nonuniversal) local fluctuations (Refs. 10 and 20) whereas the same quantity looks rather smooth when resolved on the order of the Batchelor scale (Refs. 22 and 27). This is consistent with the notion that there is no small scale intermittency in the scale range between Kolmogorov and Batchelor scales. Note that the smallest scales for the temperature fluctuation are of the order of the Kolmogorov scale, and are therefore subject to the same type of small-scale intermittency as that of the dye fluctuations near the Kolmogorov scale.

D. Reasons for differences in the shapes of E_χ between wakes and jets

It thus appears that the primary difference between the wake data and the jet data is the absence of the peak at low concentration values. This cannot be attributed to the possibility that the outside fluid never penetrates the centerline: Outer intermittency measurements (as well as the pdf measurements of the dye concentration c) suggest that the outer fluid does penetrate the jet centerline—in fact, somewhat *more* frequently than for the wake for the Reynolds numbers under consideration here. From the earlier discussion, it would appear that the reasons for this particular difference cannot reside in the Taylor's hypothesis, differences in the diffusion coefficients, or the measurement resolution.

The explanation for this differences is likely to be due to some basic physical mechanism in the two flows. This is evident in the pdf of the scalar itself. The cold side of the wake has a relatively large exponential pdf for the scalar and the conditioned expectations in this region shows a peak. The low concentration side of the jet does not show such extensive exponential region. For a simple-minded explanation for this difference in the pdf's on the low concentration end, consider the following argument. The width δ of the two-dimensional wake is of the order $x^{1/2}$ and the mean convection velocity \bar{U} does not change much across the wake. Hence, the mean concentration drops off roughly as $1/(\delta\bar{U})$ or as $x^{-1/2}$. The round jet spreads linearly and the centerline velocity \bar{U} drops off as x^{-1} . Hence, the mean concentration drops off as $1/(\delta^2\bar{U})$ or as x^{-1} . The mean concentration in the jet will therefore be substantially closer to the zero concentration of the freestream than is likely to be the case for the wake. This means that the lower cut off for the scalar pdf in the jet will be closer to the mean scalar level, so that an extensive exponential region seen in Fig. 1(c) for the wake cannot occur for the jet.

We argued that a definite relation exists between the scalar pdf and the conditioned expectation of the dissipation. There are several measures of the correlation between χ and θ as a bulk description of this interrelationship. One of these is the correlation $\langle\theta\chi\rangle$ between χ and θ . Another

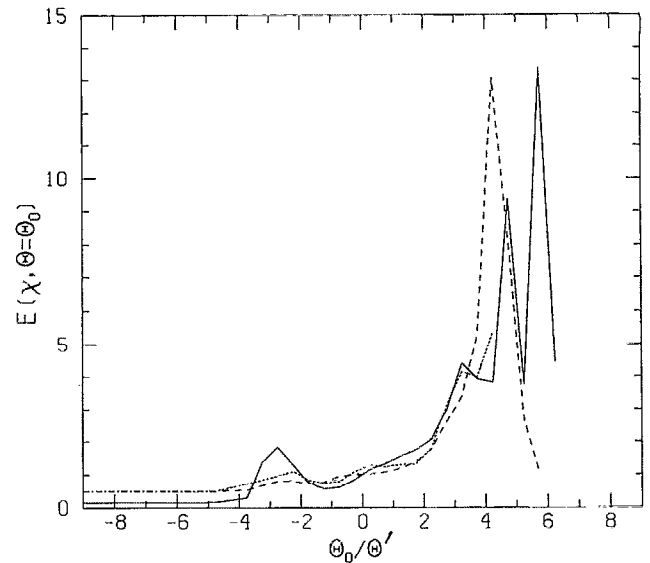


FIG. 8. Conditional expectation of the scalar dissipation for temperature fluctuations in the atmosphere. The microscale Reynolds number is estimated to be $2000 \pm 15\%$. Data selections: —, L; ---, M; ···, H.

is a pseudocorrelation coefficient $\rho = \langle\theta^2\chi\rangle$. Yet another is $\rho_p = \langle\theta^2\chi\rangle - 1$. Such measurements have been made by various workers (e.g., Refs. 16 and 28).

V. RESULTS FOR THE BOUNDARY LAYER

The main purpose of the atmospheric measurements was to obtain E_χ in a high-Reynolds-number flow. Figure 8 shows the distribution of E_χ from various selections of temperature data from the atmospheric boundary layer. These figures show a strong lobe in E_χ on the hot end with a tendency towards a far weaker peak on the cold end. Clearly, the data indicate that the structure of the dissipation at the low scalar fluctuations is different from that at high levels of fluctuations.

VI. BRIEF DISCUSSION OF RESULTS AND CONCLUSIONS

The conditional dissipation rate has been measured in three types of turbulent shear flows: Heated wakes, dyed liquid jets and the atmospheric surface layer. This expected value depends fairly strongly on the scalar value and also on the flow itself. For the wake, E_χ exhibits two broad peaks of different nature, separated by an approximately flat region: The peak near low values of the scalar correspond to the unmixed or partially mixed fluid from outside, while that near high scalar values corresponds to the well-mixed fluid. The lower peak becomes weaker for off-axis position across the wake. While the lower cutoff for E_χ is well defined, the upper cutoff corresponding to the larger concentrations is not. The latter depends on many details including the record length; in particular, it does not seem to have a smooth cutoff.

The experimental results obtained in Ref. 16 in grid-generated homogeneous turbulence also show somewhat similar lobe structure, and their relative strength depends

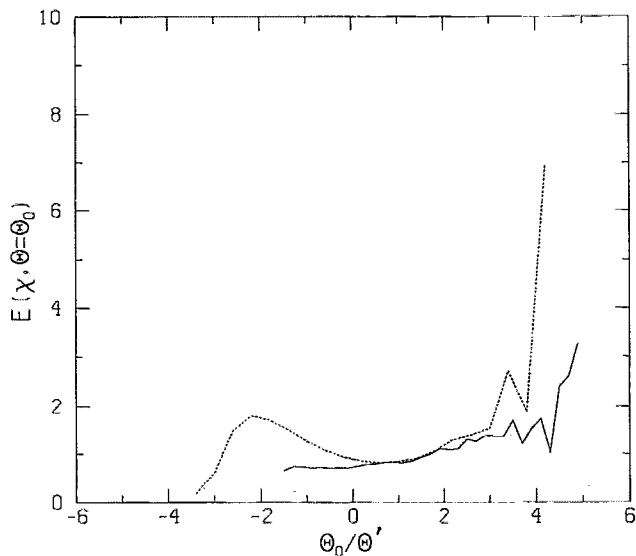


FIG. 9. Conditional expectation of the scalar dissipation in the wake at $y/l=0.13$. \cdots , for the complete signal; $---$, for temperatures above the local mean.

on whether or not there is a mean temperature gradient. The numerical results of Ref. 6 and 9 also show roughly similar effects. It is thus useful to measure $E(\chi, \theta = \theta_0)$ only for the turbulent part in the flows considered here, since it is well known that homogeneity is a better approximation in those regions. This, however, is quite difficult. As a crude (and far from satisfactory) experiment, suppose that we arbitrarily agree to designate that fluid parcels with temperatures above the local mean are fully mixed and turbulent. The $E(\chi, \theta = \theta_0)$ recomputed for the fully turbulent parcels of fluid so defined is compared in Fig. 9 with the original E_χ plot for one off-axis position in the wake. The fully turbulent curve shows a weakened lower lobe, but a nontrivial dependence on the scalar concentration.

Finally, the expected value $E_{\theta'}$ has a simpler behavior than E_χ , and may therefore be a more useful quantity to model.

With respect to other shear flows, it appears that the upper lobe is the common aspect of all conditional dissipation measurements. In particular, the absence of the lower lobe for the concentration field in water jets is attributed to the different nature of the pdf of scalar fluctuation in this region from that for the wake. It is demonstrated that the application of Taylor's hypothesis has measurable effects on the high concentration end, although the overall shape of the distribution is not affected. The use of one component of the scalar dissipation instead of the sum of all three of its components does not seem to have a significant effect on the overall shape of the conditional expectation.

As already remarked, the shape of the upper lobe for the wake is not truncated smoothly. This is so also for jets when the measurement resolution for the dissipation is comparable to the Kolmogorov scale. It is well known that the scalar dissipation for the high-Schmidt-number dyes

extends to fine scales of the order of the Batchelor scale. When these scales are resolved, the large uncertainties prevalent in the upper lobe seem to diminish (Fig. 7). This is believed to be due to the fact that the scalar dissipation in the sub-Kolmogorov scale range is nonintermittent (Refs. 22 and 27), while the same quantity coarse grained on scales of the order of the Kolmogorov scale displays high degree of intermittency and nonuniversality of extremely active events (Refs. 10 and 20). This difference in the dissipation appears to be responsible for the differences observed in Fig. 7 for the upper lobe structure.

The boundary layer data for temperature show signs of having both lobes, but that for the lower temperature is far weaker. It should again be remarked that the temperature dissipation here is highly intermittent, and the observed uncertainties in the upper lobe are consistent with this behavior.

Finally, while conditional expectation measurements of the sort presented here (or the joint probability densities of the scalar and its three gradients presented in Refs. 10 and 29) are no doubt useful, the measurement of only E_χ in inhomogeneous turbulent flows, without knowing the behavior of the conditional convective terms with which they must balance on the whole, is a little unsatisfactory.³⁰ This, however, is work for the future.

ACKNOWLEDGMENTS

We thank Professors R. W. Bilger and E. E. O'Brien for useful discussions spanning several years. To them and to Professor S. B. Pope, we are thankful for comments on an earlier draft. We thank Dr. R. R. Prasad who acquired the data for jet R and Dr. Don Aylor of the Connecticut Agricultural Research Station who helped us in acquiring the atmospheric data.

The work was supported by the Air Force Office of Scientific Research.

- ¹S. B. Pope, "The probability approach to the modelling of turbulent reacting flows," *Combust. Flame* **27**, 299 (1976).
- ²R. W. Bilger, "Turbulent flows with non-premixed reactants," in *Turbulent Reacting Flows*, edited by P. A. Libby and F. A. Williams (Springer-Verlag, New York, 1980), pp. 65-113; "Conditional moment closures for turbulent flows," *Phys. Fluids A* **5**, 436 (1993).
- ³E. E. O'Brien, "The probability density function approach to reacting turbulent flows," in *Turbulent Reacting Flows*, edited by P. A. Libby and F. A. Williams (Springer-Verlag, New York, 1980), pp. 185-218.
- ⁴S. B. Pope, "PDF methods for turbulent reactive flows," *Prog. Energy Combust. Sci.* **11**, 119 (1985).
- ⁵V. R. Kuznetsov and V. A. Sabel'nikov, *Turbulence and Combustion* (Hemisphere, New York, 1990), Chaps. 2 and 3, pp. 41-122.
- ⁶V. Eswaran and S. B. Pope, "Direct numerical simulations of the turbulent mixing of a passive scalar," *Phys. Fluids* **31**, 506 (1988).
- ⁷Y. G. Sinai and V. Yakhot, "Limiting probability distributions of a passive scalar in a random velocity field," *Phys. Rev. Lett.* **63**, 1962 (1989).
- ⁸F. Gao, "An analytical solution for the scalar probability density function in homogeneous turbulence," *Phys. Fluids A* **3**, 511 (1991).
- ⁹F. Gao and E. E. O'Brien, "Joint probability density function of a scalar and its gradient in isotropic turbulence," *Phys. Fluids A* **3**, 1625 (1991).
- ¹⁰R. R. Prasad and K. R. Sreenivasan, "Quantitative three-dimensional imaging and the structure of passive scalar fields in fully turbulent flows," *J. Fluid Mech.* **216**, 1 (1990).
- ¹¹K. R. Sreenivasan, R. A. Antonia, and H. Q. Danh, "Temperature

- dissipation fluctuations in a turbulent boundary layer," *Phys. Fluids* **20**, 1238 (1977).
- ¹²L. W. B. Browne, R. A. Antonia, and D. A. Shah, "Turbulent energy dissipation in a wake," *J. Fluid Mech.* **179**, 307 (1987).
- ¹³J. L. Lumley, "Interpretation of time spectra measured in high-intensity shear flows," *Phys. Fluids* **8**, 1056 (1965).
- ¹⁴A. S. Monin and A. M. Yaglom, *Statistical Fluid Mechanics, Vol. II* (MIT Press, Cambridge, MA, 1971).
- ¹⁵R. A. Antonia, A. J. Chambers, and N. Phan-Thien, "Taylor's hypothesis and spectra of velocity and temperature derivatives in a turbulent shear flow," *Boundary-Layer Meteorol.* **19**, 19 (1980).
- ¹⁶Jayesh and Z. Warhaft, "Probability distribution, conditional dissipation, and transport of passive temperature fluctuations in grid generated turbulence," *Phys. Fluids A* **4**, 2292 (1992).
- ¹⁷K. R. Sreenivasan, "On local isotropy of passive scalars in turbulent flows," *Proc. R. Soc. London Ser. A* **434**, 165 (1991).
- ¹⁸K. R. Sreenivasan, "Approach to self-preservation in plane turbulent wakes," *AIAA J.* **18**, 1365 (1981).
- ¹⁹R. Peattie, "A simple, low-drift circuit for measuring temperatures in fluids," *J. Phys. E* **20**, 565 (1987).
- ²⁰R. R. Prasad and K. R. Sreenivasan, "The measurement and interpretation of fractal dimensions of the scalar interface in turbulent flows," *Phys. Fluids A* **2**, 792 (1990).
- ²¹J. R. Saylor and K. R. Sreenivasan, "Differential diffusion in high Schmidt number, low Reynolds number jets," submitted for publication (1993).
- ²²K. R. Sreenivasan and R. R. Prasad, "New results on the fractal and multifractal structure of the large Schmidt number passive scalars in fully turbulent flows," *Physica D* **38**, 322 (1989).
- ²³J. C. LaRue and P. A. Libby, "Temperature fluctuations in the plane turbulent wake," *Phys. Fluids* **17**, 1954 (1974).
- ²⁴R. W. Bilger, R. A. Antonia, and K. R. Sreenivasan, "Determination of intermittency from the probability density function of a passive scalar," *Phys. Fluids* **19**, 1471 (1976).
- ²⁵V. Yakhot, "Probability distributions in high-Rayleigh-number Bénard convection," *Phys. Rev. Lett.* **63**, 1965 (1989).
- ²⁶We thank Professor S. B. Pope for bringing this relation to our attention.
- ²⁷W. J. A. Dahm, L. K. Su, and K. B. Southerland, "A scalar imaging velocimetry technique for fully resolved four-dimensional vector velocity field measurements in turbulent flows," *Phys. Fluids A* **4**, 2191 (1992).
- ²⁸F. Anselmet and R. A. Antonia, "Joint statistics between temperature and its dissipation in turbulent jet," *Phys. Fluids* **28**, 1048 (1985).
- ²⁹F. Anselmet, H. Djeridi, and L. Fulachier, "Joint statistics between a passive scalar and its dissipation in a turbulent boundary layer," in *Proceedings of the 8th Symposium on Turbulent Shear Flows, Munich, 1991*, pp. 27-3-1-27-3-6.
- ³⁰Private communication, June 1992.